Ocean Warming of Nares Strait Bottom Waters off NW Greenland 2003-09

A. Münchow

College of Earth, Ocean and Environment, University of Delaware, Newark, Delaware, USA

K. K. Falkner

National Science Foundation, Arlington, Virginia, USA

H. Melling

Institute of Ocean Sciences, Department of Fisheries and Oceans, Sidney, British Columbia, Canada

B. Rabe

Marine Laboratory, Marine Scotland - Science, Aberdeen, United Kingdom

H. L. Johnson

Department of Earth Sciences, University of Oxford, Oxford, United Kingdom

Instead of a hostile, sluggish, steady, ice-covered environment with little impact on the global ocean, the Arctic is becoming an increasingly accessible, rapidly changing, dynamic, and only partly ice-covered ocean that is implicated in global climate and environmental change. More specifically, our new observations demonstrate that waters off northwest Greenland constitute the final limb in the grand cyclonic circulation of the Atlantic layer in the Arctic Ocean. These waters with an Atlantic water mass signature are warming in Nares Strait to the west of Greenland as they are elsewhere. Estimates of the magnitude and uncertainty and indications of the dynamics and downstream consequences of this warming are emerging from both our moored observations and historical hydrographic station data.

Ocean temperatures sensed by instruments moored 3-m above the bottom between 228 to 366 meter depth in Nares Strait suggest a mean warming of about 0.023 ± 0.015 °C per year for the 2003 through 2009 period at 95% confidence. Salinity changes for the same period are not significantly different from zero. Nevertheless, oscillating bottom temperatures co-vary with salinities. Mean bottom salinities in Nares Strait exceed 34.56 psu while no

---

A. Münchow, 112 Robinson Hall, College of Earth, Ocean and Environment, University of Delaware, Newark, Delaware, USA. (muenchow@udel.edu)

water with salinities above 34.51 psu occurs in Baffin Bay to the south. This indicates a dominantly northern source for the waters sensed by our moorings. Mean bottom temperatures hover near 0°C which suggests minimal influence of waters from the northeastern Amundsen Basin in the Arctic Ocean. We thus conclude that the observed warming originates from the northeastern Canadian Basin to the south-west of our study area.

In addition to these mean conditions, we find large interannual variability. For example, significant freshening emerges for the 2003-06 period that reaches -0.02 ± 0.008 psu per year without significant concurrent temperature trends at three sensor locations. This contrasts with the 2007-09 observational period when five different sensors all indicate warmer waters (0.063 ± 0.017 °C per year) and saltier waters (0.027 ± 0.01 psu per year) which reverses the 2003-06 freshening. We speculate that some of these observed changes are caused by a changing ice regime. During the 2003-06 winters ice was landfast while during 2007-09 it was generally mobile year-round. The warming impacts tidewater glaciers along northern Greenland with sill depths below 300 m, e.g., Petermann Gletscher.

1. Introduction

When a large outlet glacier of northwest Greenland (Petermann Gletscher) discharged an ice island four times the size of Manhattan in August of 2010, the United States' Congress held formal inquiries on its cause within days of the event. Some scientists and the global media speculated that this event as well as concurrent severe droughts in Russia and floods in China and Pakistan were tied to record breaking air temperatures and global warming. Reviewing available data, *Johnson et al.* [2011] and *Falkner et al.* [2011] cautioned that most melting of floating ice shelves such as Petermann Gletscher is dominated by physical ocean processes below, not above the ice [*Rignot and Steffen*, 2008]. We here provide evidence that waters adjacent to Petermann Gletscher (a) originate from the Arctic Ocean to the north, (b) contain heat of Atlantic origin, and (c) have warmed significantly since 2003.

Changing ocean properties are observed in the Eurasian [*Polyakov et al.*, 2010] and North-American [*McLaughlin et al.*, 2009; *Melling*, 1998] sectors of the Arctic Ocean in recent years. The Arctic Ocean and its marginal seas have pronounced subsurface temperature maxima [*Coachman and Barnes*, 1963] on account of inflowing warm and salty Atlantic waters. These enter via eastern Fram Strait [*Fahrbach et al.*, 2001] and the Barents Sea [*Schauer et al.*, 2002]. The circulation of the central Arctic Ocean is generally cyclonic (counter-clockwise) and most intense near boundaries adjacent to sloping topographic features [*Nikolopoulos et al.*, 2008]. It is explained elegantly by vorticity conservation in the presence of a wind-stress curl [*Yang*, 2005]. Atlantic layer core temperatures in the Arctic vary from 4 °C in the generally ice-free Barents Sea [*Levitus et al.*, 2009] to below 0.5 °C in the generally ice-covered eastern Canadian Basin [*McLaughlin et al.*, 2009; *Melling*, 1998].

The Canadian Archipelago, Fram Strait, and Barents Sea constitute pathways of water, ice, and vorticity between the Arctic and Atlantic Oceans. Arctic outflows via these pathways return freshwater to the North Atlantic that was evaporated from tropical oceans, transported by the atmosphere, and delivered to the Arctic Ocean via precipitation, terrestrial run-off, and inflow from the North Pacific [*Emile-Geay et al.*, 2003]. We here focus on changing water properties in Nares Strait to the west of Greenland bordering the Canadian Archipelago [*Münchow et al.*, 2007]. Nares Strait is a major conduit of southward flux into Baffin Bay and the Atlantic Ocean [*Münchow and Melling*, 2008]. Fluxes and properties through Nares Strait reflect the impacts of disintegrating ice shelves of northern Canada [*Copland et al.*, 2007], potentially surging glaciers of northern Greenland [*Rignot and Steffen*, 2008; *Johnson et al.*, 2011], and diminishing sea ice in the Arctic [*Parkinson and Cavalieri*, 2008].

Since the Lincoln Sea to the north of Greenland and Ellesmere Island contains some of the oldest and thickest ice anywhere in the Arctic Ocean, the circulation and properties of its underlying waters impact the fate of these last remains of multi-year ice. The flux of such ice is currently limited to a 3-4 month long summer season. For the remainder of the year, the ice is land-fast, but the duration of these conditions are changing [*Kwok et al.*, 2010]. More specifically, the length of the land-fast ice season in winter is decreasing. Processes within and adjacent to the Canadian Archipelago strongly link ice, ocean, and land in a system that conceivably moves more multi-year ice from the Arctic than is currently possible during a 3-4 month season of ice mobility.

Subsurface Arctic Ocean temperature records longer than 80 years reveal both multi-decadal oscillations [*Levitus et al.*, 2009; *Polyakov et al.*, 2004] and smaller, but significant linear trends of increasing temperatures [*Polyakov et al.*, 2004; *Zweng and Münchow*, 2006]. Analyses of discrete hydrographic ship surveys such as those cited are challenged by seasonally biased sampling, gappy records, and aliasing introduced by unresolved spatial and temporal variabilities of a dynamical ice-ocean-atmosphere system [*Wunsch and Heimbach*, 2006]. In contrast, generally shorter mooring records sample more frequently and regular, thus contain less bias, but to date are shorter than a decade.

We here introduce temperature and salinity measurements from moorings that describe means, variability, and trends from super-tidal to interannual time scales near the bottom at several locations across a 38 km wide section of Nares Strait from 2003 to 2009. After introducing our study area to the west of Greenland, we place our moored measurements into a larger spatial context with discrete vertical profiles collected from ships and helicopters in 2003. Time series of bottom temperature and salinity are analyzed for dominant time scales of variability as well as for linear trends that constitute a first estimate of variations at decadal time scales. We discuss our findings in the context of both multi-decadal oscillations and a potential regime change towards an Arctic with a more seasonal and mobile ice cover.

2. Data sources

Starting in 2003, we measured ocean properties in Nares Strait, a 30-50 km wide waterway that separates Greenland from Canada between 78°N and 83°N latitudes (Fig. 1). To the north it connects to the Arctic Ocean, while to the south it connects to Baffin Bay and subsequently the Atlantic Ocean. At 80.5°N latitude we deployed an array of moorings to measure ocean currents, temperature, and conductivity across a 38 km wide and 350 m deep section of Nares Strait. *Münchow and Melling* [2008] and *Rabe et al.* [2010] introduced details and first results from instruments measuring ocean currents between 30 m and 300 m depth and temperature, conductivity, and pressure between 30 m depth and a few meters above the seabed for the 2003 through 2006 period. The instruments recovered in 2006 and 2009 provide gap-free records that are two and three years long, respectively. We here report for the first time on interannual temperature and salinity changes for the 2003 through 2009 period.

Bottom-mounted SeaBird 37SM sensors reveal temperature and salinity about three meters above the bottom where turbulence levels, biological activity, and mooring motions are all smaller than in the water column above. Samples were taken every 15 minutes. Salinity is estimated from conductivity, temperature, and pressure. We estimate temporal sensor drift by comparing 20 days of mooring records at the start and the end of the series with discrete vertical CTD profiles taken during deployment and recovery operations. Assuming negligible drift of temperature sensors, we find (not shown) that salinities drift by about 0.051 psu towards fresher values for the 2003-06 period (-0.017 psu/year) and 0.031 psu towards fresher values also for the 2007-09 period (-0.016 psu/year). The sign and magnitude of these changes is consistent with gradual fouling of a conductivity cell. This constant salinity drift is removed from the 2003-06 records at KS02, KS10, and KS12 as well as from the 2007-09 records at KS04, KS06, KS08, KS10, and KS12 (see Fig. 1 for locations).

Of the eight separate time series of salinity S, only two records contain salinity spikes with $S < 34.1$. Both occur at KS10 with the first starting May-16, 2005 lasting for 18 days and the second starting November-26, 2008 lasting 0.25 days. We replaced these anomalous salinities with values estimated from a linear regression of salinity against temperature ten days prior. As a final processing step we apply a Lanczos raised cosine low-pass filter with a half-power point near 34 hours to remove tidal and inertial variations. Uncertainties on statistical estimates require knowledge of the degrees of freedom which is the ratio of the record length T to the decorrelation time scale Td. We determine Td by integrating lagged auto-correlations of salinity and temperature to their first zero crossing and find Td in the range of 5-14 days (not shown). Using Td=14 days our 2003-06 and 2007-09 records have about 78 and 51 degrees of freedom.

3. Spatial Context

Fig. 1 shows the location of our larger study area from the 4000-m deep Amundsen Basin and 1500-m deep Lomonosov Ridge in the Arctic Ocean at 89°N latitude to the 2000-m deep Baffin Bay basin at 73°N latitude. Nares Strait connects these two basins with northern and southern sill depths near 84°N and 80°N latitude of about 300 m and 200 m depth, respectively. Fig. 1 also shows the location of five CTD casts that were taken in Nares Strait between its northern and southern sills as well as stations bordering the adjacent deep basins to the north and south of the sills. Fig. 2 depicts vertical profiles of salinity from 150-m below the surface to the bottom near 500-m depth. Below the main halocline at any given depth it clearly shows the progression of high salinities in the Arctic Ocean to lower salinities in Nares Strait and to the lowest salinities in Baffin Bay. Except for Baffin Bay, the correlation of salinity S with potential temperature θ is almost linear (Fig. 3) as temperature increases with salinity. All Nares Strait waters with salinities above 34.54 are either locally produced by brine injections or must have entered from the north, because Baffin Bay waters with a subsurface temperature maximum have salinities that are always less than 34.54 [*Münchow et al.*, 2011].

The shallow Nares Strait cast terminating at 330-m depth with a bottom salinity of 34.72 originates from our mooring section while a deeper Nares Strait cast taken to the north measures salinities reaching 34.82 at 500-m. Waters with these θ-S characteristics are found at about 350-m depth in the Arctic Ocean just to the north of the northern sill. These data indicate that either an uncharted sill deeper than the charted 300-m sill exists or episodic upwelling raises the salty Arctic Ocean waters from 350-m to 300-m depth and over the sill to subsequently cascade down into Nares Strait to form Nares Strait bottom water with S=34.82 and potential temperature θ=0.20 °C. The vertical excursion would likely be larger than 50-m as the downward motion would entrain fresher water as it descends.

Besides the temperature salinity correlations from the CTD casts we also show in Fig. 3 the mean temperature and salinity values from the eight time series (Table 1) along with the magnitude of temperature and salinity changes that we discuss next . Mean values aggregate between 34.56 and 34.67 along the Arctic Ocean and Nares Strait correlations. This gives confidence that both the 2003 CTD casts as well as our mooring data represent similar waters.

4. Time Series 2003-2009

Fig. 4 shows salinity and potential temperature for the 2003-06 and 2007-09 deployments near the center of the channel at KS10 (see Fig. 1 for location). Salinity at KS10 generally varies between 34.4 and 34.7 except for two events in January 2004 (Day 366) and December 2007 (Day-1800) with unfiltered salinities reaching almost 34.3 that also correspond to lower temperatures (not shown). Temperatures are within a narrow range between -0.4 °C and +0.2 °C except for two short events. Without the hindsight of mooring data *Samelson et al.* [2006] discuss the first event in terms of strong wind-forcing and ice motion that *Rabe* [2010] analyze as a wind-driven response of a density stratified channel flow under the influence of rotation. The perhaps physically similar 2007 event of low bottom temperature and salinity also corresponds to strong winds from the north. These winds cause strong upwelling off Greenland that brings warmer waters towards the surface and advects loose ice towards the channel center and to the south [*Rabe*, 2010]. This upwelling results in large areas of active sea-ice formation that is visible in MODIS thermal imagery (Fig. 6) where high brightness temperatures indicate thermal radiation from open water or thin ice.

Note that the highest salinities with values above 34.7 occur at the beginning of the record in the summer of 2003 and the end of the record in the summer of 2009. Salinities indicate that waters become fresher in 2003 and saltier in 2009 for six to nine months.

Within a time series covering six years, such short-period trends stand out, but they are balanced by opposing trends at other times. A single year-long record, however, would potentially mis-interpret the significance of such trends that really are oscillations at time scales longer than the record. The same caveat, albeit at decadal time scales, does apply to any linear trend analysis applied to our six year period of observations.

5. Linear Regressions

Table 1 lists record mean values and salient statistics for each location for each deployment period. The linear warming and freshening during the period of observations are overlaid in Fig. 4 for the center of the channel at KS10 for potential temperature θ and salinity S both as time series and as θ-S scatter. The linear trend line for time series is shown also with values for the slopes listed in Table 1. Furthermore, we color code data prior to May-16, 2005 (Day-866) in black and those after this time in red for the 2003-06 record. While not apparent from the time series, depicting the data as θ-S scatter irrespectively of time, we show that the selected time corresponds to the arrival of a fresher and warmer water mass. More specifically, a strong linear relation exists in θ-S space, however, the relation prior and after May-16, 2005 are distinct. Furthermore, this shift occurs instantaneously at multiple bottom sensors across the section such as at KS02 adjacent to the coast of Canada (Fig. 5) and at KS12 near the coast of Greenland (not shown). This date separates a cooler-fresher water from a warmer saltier water. Similar coherent changes of water properties across the entire array occur during the 2007-09 deployments on Oct.-31, 2008 which we show in Figs. 4 and 5 for the center channel location

KS10 and a coastal Canada location KS04. Additional sensors at KS06, KS08, and KS12 show similar behavior (Table 1).

During the 2003-06 period linear trends of potential temperature are indistinguishable from zero within 95% confidence levels at all three locations across the channel (Table 1). In contrast, salinity trends indicate freshening of about 0.018 ± 0.008 psu per year at KS02 (Fig. 5). Values at all three locations are indistinguishable from each other within their respective uncertainties which is true for the 2007-09 period as well. For the latter period, however, our data suggests more dramatic rates of change in time. Both temperature and salinity trends are different from zero at 95% confidence except for one shallower location (KS12). At KS04 temperature and salinity trends exceed 0.065 ± 0.022 °C per year and 0.030 ± 0.013 psu per year (Fig 5). There is no apparent pattern in these rates from sensor to sensor across the channel. We thus assume that each record represents an independent realization of the same change. This reduces the uncertainty of the estimated across-channel averaged trends by $\sqrt{N-1}$ where N=3 for 2003-06 and N=5 for 2007-09. Sectionally averaged bottom temperature in Nares Strait thus warm by 0.027 ± 0.010 °C and become saltier by 0.063 ± 0.017 per year from 2007 to 2009.

6. Discussion

The Arctic Ocean resembles an estuary with respect to the Atlantic Ocean. As a strongly stratified ocean, it delivers relatively fresh waters to the Atlantic near the surface and in return receives relative salty waters below the surface. Both the Arctic's sea ice cover and the stability of Greenland's outlet glaciers depend on the delicate balance of the inflows and outflows and the salt and heat content that these waters carry.

Analysis of historical records report Arctic change from ship-based observations [*Levitus et al.*, 2009; *McLaughlin et al.*, 2009; *Polyakov et al.*, 2004; *Zweng and Münchow*, 2006; *Melling*, 1998] of temperature and salinity for the last 10-100 years. Most of these records contain linear trends that demonstrate subsurface warming of the Atlantic layer. The data also contain large amounts of scatter and oscillations. Furthermore, much of the sampling is seasonally biased towards the polar summers when access is easier. Few records are sampled frequently enough to resolve temporal and spatial oscillations due to Kelvin and Rossby waves [*Gill*, 1982] that have periods of days to months. And lastly, few historical records are long enough to resolve interannual and decadal oscillations of the atmospheric circulation patterns described by the North-Atlantic Oscillation [*Hurrell and Deser*, 2009] and the Atlantic Multidecadal Oscillation [*Enfield et al.*, 2001].

Exceptions are *Levitus et al.* [2009] who finds strong correlations in an almost 110-year long record of subsurface Barents Sea temperature measurements that correlate with the Atlantic Meridional Oscillation. *Polyakov et al.* [2004] reports Atlantic layer core temperatures from the slopes and basins of the Arctic ocean and also finds correlations with climate indices in addition to a weak background warming trend of 0.026 ± 0.008 °C per decade for the region to the north of Nares Strait from discrete casts covering 26 different years with data. Note that this trend is an order of magnitude smaller than what we report here for our 2003-09 mooring record and that the 26 CTD casts are widely separated in both time and space.

We here report first results from moored records that for five years resolved hourly to interannual time scales at 5-km spatial scales. Our array does not resolve decadal variability, but the linear trend represents a first estimate of long-term variability that includes both decadal variability and steady background warming or cooling. We are presently unable to distinguish between the two. Nevertheless, combining our 2003-06 and 2007-09 records from three and five sensors, respectively, we find a mean warming of about 0.023 $\pm$ 0.015 °C per year where the uncertainty represents a 95% confidence interval for a 14 day decorrelation time scale determined conservatively from the data. The salinity data reveal freshening of -0.001 $\pm$ 0.009 psu per year that is not significantly different from a zero.

The observed trends are spatially coherent across the section. The large warming by up to 0.07 °C per year starting in 2007 coincides with the arrival of waters that also have higher salinities which reversed the freshening of prior years. Water properties in Nares Strait also change at daily to interannual times scales perhaps associated with the arrival of water mass fronts in θ-S space. The timing and frequency of such occurrences contributes to the warming, however, it implies a different and potentially more dynamic and nonlinear process than a steady, uniform, and linear rise of ocean temperatures.

We present two speculations on the cause of the enhanced warming, namely (a) advection from the north and (b) local convection with attendant vertical mixing. First, warming waters of Atlantic origin previously detected in the Canadian Basin [*McLaughlin et al.*, 2009] may have reached the Lincoln Sea, pushed over the 300-m deep northern sill, and entered Nares Strait from the north. Bottom temperature and salinity in Nares Strait suggest a source for such water at 350-m depth in the Arctic Ocean. In order to enter

Nares Strait, these waters must be lifted intermittently by almost 50-m to cross the sill and plunge to the bottom of Nares Strait (Fig. 2).

A second, perhaps concurrent cause could be changing local ice conditions. More specifically, for the 2003-06 period, Nares Strait developed ice arches at its southern entrance [*Dumont et al.*, 2009] that remained in place for 158, 242, and 169 days during the 3 winters [*Kwok et al.*, 2010]. This arch locks all motion of ice in Nares Strait [*Dunbar*, 1973], decouples the ocean circulation from the local atmosphere, and supports the North Water polynya [*Melling et al.*, 2001]. The polynya failed to form in the 2006/07 winter [*Münchow et al.*, 2007] when ice was moving all year through Nares Strait from north to south. During the 2007/08 winter it lasted for only 68 days [*Kwok et al.*, 2010], and again failed to form at all in the winter of 2008/09. Instead, a northern ice arch formed on January 17, 2009 (Fig. 7) and all locally produced sea ice was promptly exported into Baffin Bay to the south. This northern ice arch formation coincided with a rapid warming observed in 2009 at all locations in Nares Strait both near the bottom (Fig. 4) and within the water column (not shown). Year-long southward advection of ice and surface waters leads to enhanced local ice production, brine rejection and entrainment of overlying warm waters as these brines sink. This process may be further enhanced during periods of strong upwelling favorable winds from the north. The offshore Ekman transport off Greenland due to winds from the north moves loose or thin ice towards the center of the channel. The thus created open waters during freezing air temperatures result in enhanced sea ice production, brine rejection and entrainment of overlying warm waters as these brines sink (Fig. 7).

MODIS thermal imaging for the 2009/10 winter (not shown) indicates that a northern ice arch similar to that shown in Fig. 7 formed intermittently without a southern ice arch. Except for a short period in 2008, a southern ice arch has been in place since Jan.-30, 2011 (not shown) for the first time since 2006 stopping all flow of ice in Nares Strait. An array of bottom moored sensors was deployed in Nares Strait in 2009 that will hopefully be recovered in 2012 to extend our ocean observations for another three years. We hypothesize that the accelerated large warming trend coincident with the failure of a southern ice arch will have continued through 2010 but will reverse in 2011. The fact that we do find statistically significant regressions indicative of freshening for the 2003-06 and increasing salinity for the 2007-09 periods should encourage (a) cautious interpretations of short records and (b) efforts to extend existing interannual observations at key locations such as Nares Strait. Such data are crucial for testing Arctic Ocean and climate models under development with sufficient resolution to more faithfully represent flows and driving forces through the Canadian Archipelago and adjacent waters.

Acknowledgments. We are grateful to the officers and crews of the USCGC Healy commanded by Captain Dan Oliver and CCGS Henry Larsen commanded by Captains John Vanthiel and John Broderick who endorsed our scientific objectives with enthusiastic professionalism as did a dedicated group of students, technicians, and engineers. The work was funded by the National Science Foundation under grants 0230236 (AM, HM, BR), 1022843 (AM), 0230354 (KKF) as well as the Canadian International Polar Year project 2006-SR1-CC-135 (HM).

References

Coachman, L., and C. Barnes, The movement of Atlantic water in the Arctic Ocean, *Arctic*, *16*, 9–16, 1963.

Copland, L., D. R. Mueller, and L. Weir, Rapid loss of the Ayles ice shelf, Ellesmere Island, Canada, *Geophys. Res. Let.*, *34*, L21,501, 2007.

Dumont, D., Y. Gratton, and T. E. Arbetter, Modeling the dynamics of the North Water polynya ice bridge, *J. Phys. Oceanogr.*, *39*, 1448–1461, 2009.

Dunbar, M., Ice regime and ice transport in Nares Strait, *Arctic*, *26*, 282–291, 1973.

Emile-Geay, J., M. A. Cane, N. Naik, R. Seager, A. C. Clement, and A. van Geen, Warren revisited: Atmospheric freshwater fluxes and "why is no deep water formed in the North Pacific", *J. Geophys. Res.*, *108*, 3178, 2003.

Enfield, D. B., A. M. Mestas-Nunez, and P. J. Trimble, The Atlantic multidecadal oscillation and its relation to rainfall and river flows in the continental US, *Geophys. Res. Let.*, *28*, 2077–2080, 2001.

Fahrbach, E., J. Meincke, S. Osterhus, G. Rohardt, U. Schauer, V. Tverberg, and J. Verduin, Direct measurements of volume transports through Fram Strait, *Polar Research*, *20*, 217–224, 2001.

Falkner, K., et al., Context for the recent massive Petermann Glacier calving event, *EOS*, *92*, 117–124, 2011.

Gill, A., *Atmosphere-Ocean Dynamics*, Academic Press Inc., 1982.

Hurrell, J. W., and C. Deser, North Atlantic climate variability: The role of the North Atlantic Oscillation, *J. Mar. Sys.*, *78*, 28 – 41, 2009.

Johnson, H., A. Münchow, K. Falkner, and H. Melling, Ocean circulation and properties in Petermann Fjord, Greenland, *J. Geophys. Res.*, *116*, C01,003, 2011.

Kwok, R., L. T. Pedersen, P. Gudmandsen, and S. S. Pang, Large sea ice outflow into the Nares Strait in 2007, *Geophys. Res. Let.*, *37*, L03,502, 2010.

Levitus, S., G. Matishov, D. Seidov, and I. Smolyar, Barents Sea multidecadal variability, *Geophys. Res. Let.*, *36*, L19,604, 2009.

McLaughlin, F. A., E. C. Carmack, W. J. Williams, S. Zimmermann, K. Shimada, and M. Itoh, Joint effects of boundary currents and thermohaline intrusions on the warming of Atlantic water in the Canada Basin, 1993-2007, *J. Geophys. Res.*, *114*, C00A12, 2009.

Melling, H., Hydrographic changes in the Canada Basin of the Arctic Ocean, 1979-1996, *J. Geophys. Res.*, *103*, 7637–7645, 1998.

Melling, H., Y. Gratton, and G. Ingram, Ocean circulation within the North Water polynya of Baffin Bay, *Atmos.-Oceans*, *39*, 301–325, 2001.

Münchow, A., and H. Melling, Ocean current observations from Nares Strait to the west of Greenland: Interannual to tidal variability and forcing, *J. Mar. Res.*, *66 (6)*, 801–833, 2008.

Münchow, A., K. Falkner, and H. Melling, Spatial continuity of measured seawater and tracer fluxes through Nares Strait, a dynamically wide channel bordering the Canadian Archipelago, *J. Mar. Res.*, *65 (6)*, 759–788, 2007.

Münchow, A., K. Falkner, and H. Melling, Baffin Island and West Greenland Current systems in northern Baffin Bay: Synoptic observations and climatological context, *J. Phys. Oceanogr.*, *submitted*, xxx, 2011.

Nikolopoulos, A., R. Pickart, P. Fratantoni, K. Shimada, D. Torres, and E. Jones, The western Arctic boundary current at 152° W: Structure, variability, and transport, *Deep-Sea Res.*, 2008.

Parkinson, C. L., and D. J. Cavalieri, Arctic sea ice variability and trends, 1979-2006, *J. Geophys. Res.*, *113*, C07,003, 2008.

Polyakov, I. V., G. V. Alekseev, L. A. Timokhov, U. S. Bhatt, R. L. Colony, H. L. Simmons, D. Walsh, J. E. Walsh, and V. F. Zakharov, Variability of the intermediate Atlantic water of the Arctic Ocean over the last 100 years, *J. Clim.*, *17*, 4485–4497, 2004.

Polyakov, I. V., et al., Arctic ocean warming contributes to reduced polar ice cap, *J. Phys. Oceanogr.*, *40*, 2743–2756, 2010.

Rabe, B., Dynamical analysis of flows through Nares Strait, between the Canadian Arctic Archipelago and NW Greenland, Ph.D. thesis, University of Delaware, 2010.

Rabe, B., A. Münchow, H. Johnson, and H. Melling, Nares Strait hydrography and salinity field from a 3-year moored array, *J. Geophys. Res.*, *115*, 2010.

Rignot, E., and K. Steffen, Channelized bottom melting and stability of floating ice shelves, *Geophys. Res. Let.*, *35*, L02,503, 2008.

Samelson, R. M., T. Agnew, H. Melling, and A. Münchow, Evidence for atmospheric control of sea-ice motion through Nares Strait, *Geophys. Res. Let.*, *33*, L02,506, 2006.

Schauer, U., H. Loeng, B. Rudels, V. K. Ozhigin, and W. Dieck, Atlantic Water flow through the Barents and Kara Seas, *Deep-Sea Res.*, *49*, 2281–2298, 2002.

Wunsch, C., and P. Heimbach, Estimated decadal changes in the North Atlantic meridional overturning circulation and heat flux 1993-2004, *J. Phys. Oceanogr.*, *36*, 2012–2024, 2006.

Yang, J. Y., The Arctic and subarctic ocean flux of potential vorticity and the Arctic Ocean circulation, *J. Phys. Oceanogr.*, *35*, 2387–2407, 2005.

Zweng, M. M., and A. Münchow, Warming and freshening of Baffin Bay, 1916-2003, *J. Geophys. Res.*, *111*, C07,016, 2006.

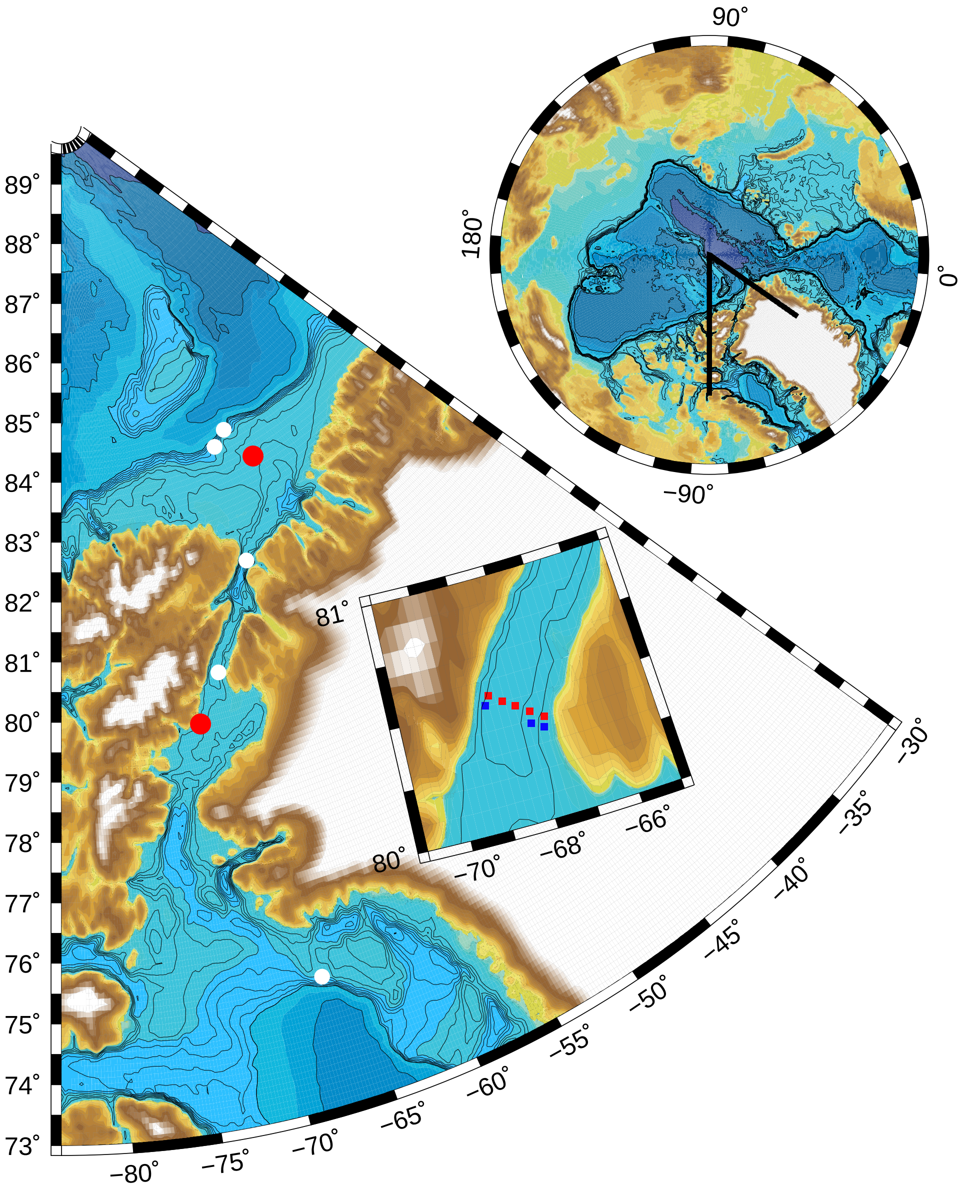

Figure 1. Maps of the Arctic Ocean (top right) and the Nares Strait (bottom left) study area with bottom contours from IBCAO in meters with contours every 100-m from 200-m to 1000-m and 1000-m beyond that depth. Sill locations are indicated with large red circles in the north (290-m) and south (225-m). White circles indicate locations of selected 2003 CTD casts. The inset near 80.5° N latitude indicates bottom-mounted ADCP mooring locations for 2003-06 (blue symbols for KS02, KS10, KS12 from west to east) and 2007-09 (red symbols for KS04, KS06, KS08, KS10, and KS12 from west to east), the symbols for the 2003-06 mooring locations are offset by 0.05 degrees latitude from their true location for clarity.

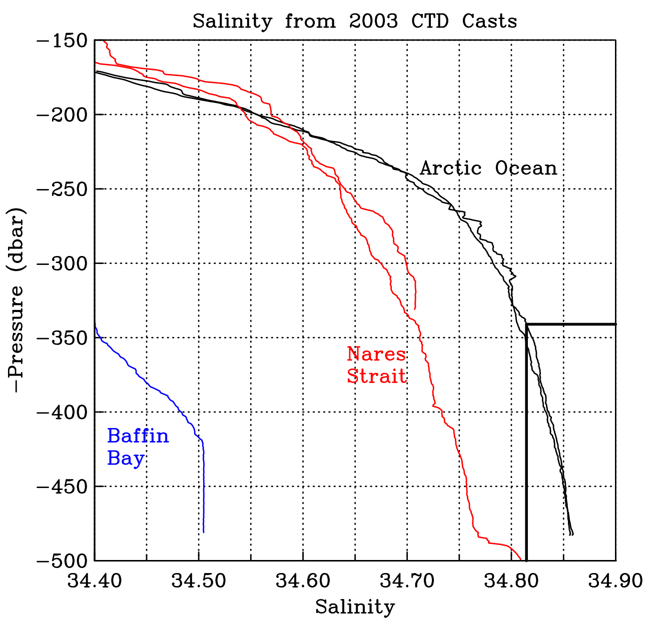

Figure 2. Vertical salinity profiles below 150-m from the Arctic Ocean to the north of the northern sill (black), Nares Strait between the northern and southern sill (red), and Baffin Bay to the south of the southern sill (blue). See Fig. 1 for locations. The Nares Strait profile terminating near 330 dbar originates from our mooring section while the profile terminating at 500 dbar is to the north where we find the densest water in 2003 (σ_θ=27.94 $kg\,m^{-3}$, S=34.82 psu).

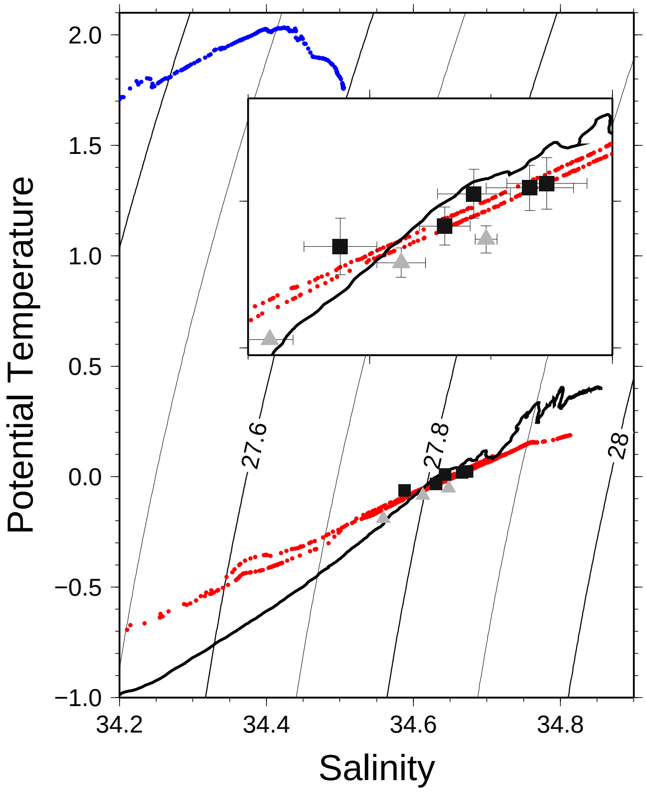

Figure 3. Temperature-Salinity correlations from the Arctic Ocean to the north of the northern sill (black), Nares Strait between the northern and southern sill (red), and Baffin Bay to the south of the southern sill depth (blue). Symbols represent record mean properties of eight mooring records in the range [34.56, 34.67] psu for salinity and [-0.19, +0.10] °C for temperature (Table 1) with triangles from the 2003-06 and rectangles from the 2007-09 deployment. See Fig. 1 for locations. Contours are lines of constant density. The insert is an expanded view where the uncertainties represent changes about the mean associated with changes discussed in the text.

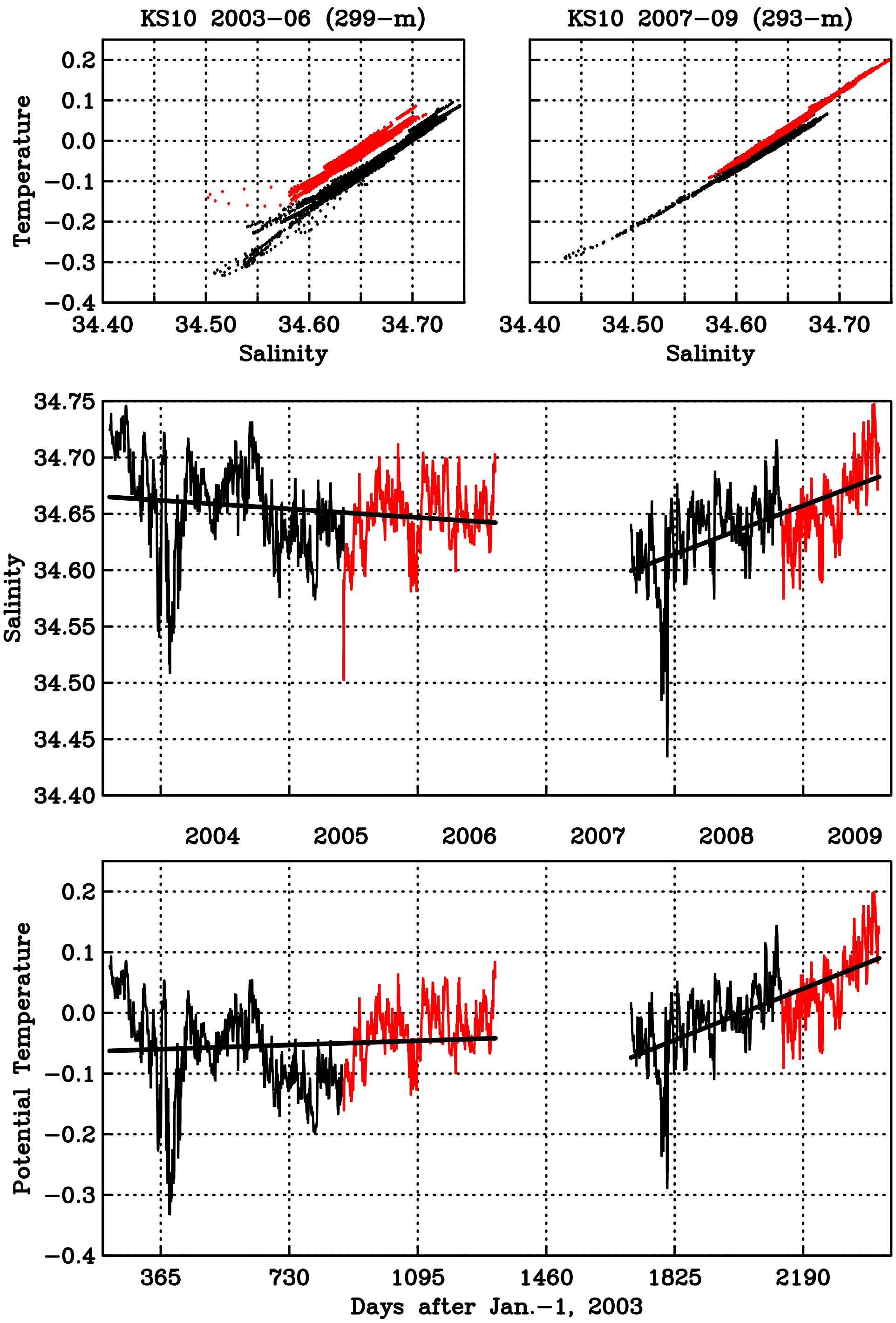

Figure 4. Time series and correlations of salinity and potential temperature near the bottom at KS10. Data are low-pass filtered to remove tidal and inertial variability. Different colors indicate data relative to events discussed in the text.

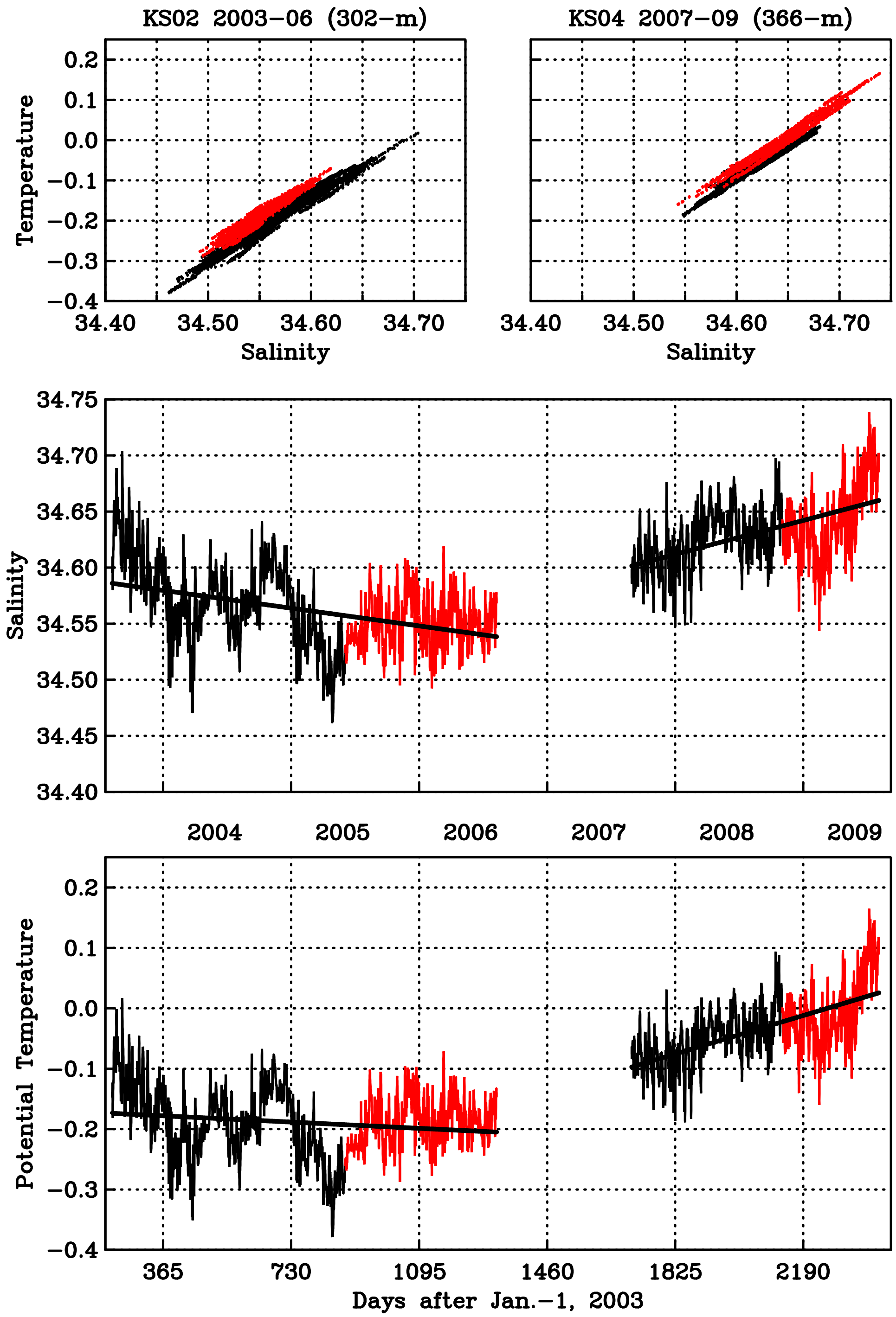

Figure 5. Time series and correlations of salinity and potential temperature near the bottom at KS02 for 2003-06 and KS04 for 2007-09. Data are low-pass filtered to remove tidal and inertial variability. Different colors indicate data relative to events discussed in the text.

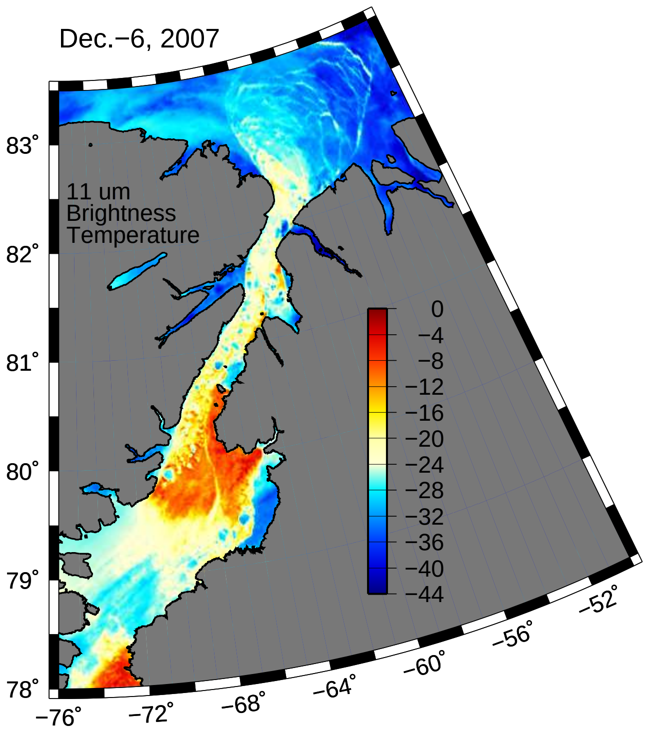

Figure 6. Brightness temperature at 11 μm from MODIS Terra on Dec.-6, 2007 (Day-1800 in Fig. 4) showing a large area of high temperatures near our mooring section at 80.5° N that represents thermal radiation from either open water or very thin ice.

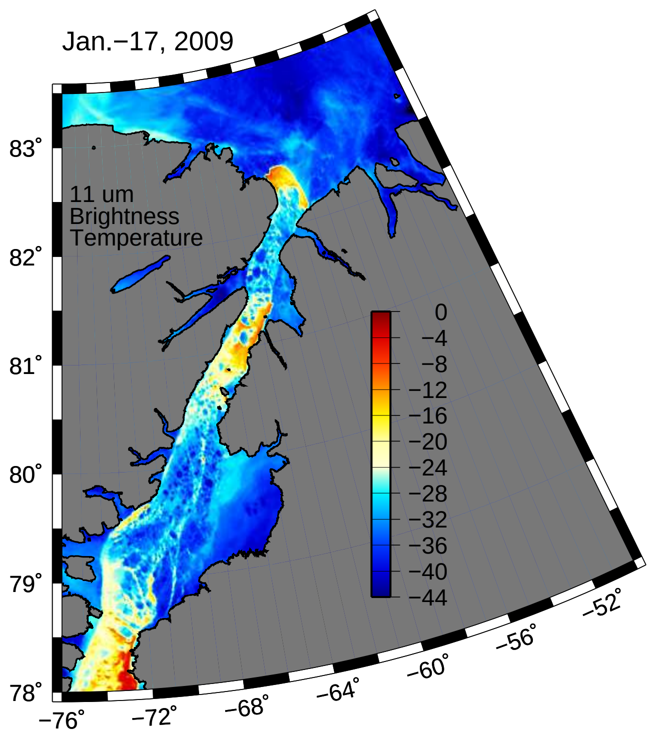

Figure 7. Brightness temperature at 11 um from MODIS Terra on January 17, 2009.

Table 1. Mooring details, averaged temperature Tbar and salinity Sbar, linear trend for temperature dT/dt and salinity dS/dt along with 95% confidence levels assuming a 14 day decorrelation time scale resulting in 78 and 51 degrees of freedom for the 2003-06 and 2007-09 deployments, respectively.

Name	Lon., W	Lat., N	Depth, m	Tbar, psu	Sbar, °C	dT/dt, °C/year	dS/dt, psu/year
KS02 2003-06	68.8744	80.5538	302	-0.19	34.56	-0.010 ± 0.014	-0.018 ± 0.008
KS10 2003-06	67.9296	80.4388	299	-0.05	34.65	+0.000 ± 0.020	-0.015 ± 0.010
KS12 2003-06	67.6709	80.4092	263	-0.08	34.61	+0.001 ± 0.025	-0.026 ± 0.014
KS04 2007-09	68.7393	80.5378	366	-0.03	34.64	+0.065 ± 0.022	+0.030 ± 0.013
KS06 2007-09	68.4555	80.5038	358	+0.02	34.67	+0.063 ± 0.028	+0.035 ± 0.016
KS08 2007-09	68.1850	80.4715	356	+0.02	34.67	+0.066 ± 0.029	+0.028 ± 0.017
KS10 2007-09	67.8930	80.4355	293	+0.01	34.64	+0.059 ± 0.037	+0.023 ± 0.022
KS12 2007-09	67.5927	80.3993	228	-0.06	34.59	+0.064 ± 0.047	+0.019 ± 0.030